JCI The Journal of Clinical Investigation

Peripheral host T cells survive hematopoietic stem cell transplantation and promote graft-versus-host disease

Sherrie J. Divito, … , Frode L. Jahnsen, Thomas S. Kupper

J Clin Invest. 2020;130(9):4624-4636. https://doi.org/10.1172/JCI129965.

Research Article | Immunology | Transplantation

Graphical abstract

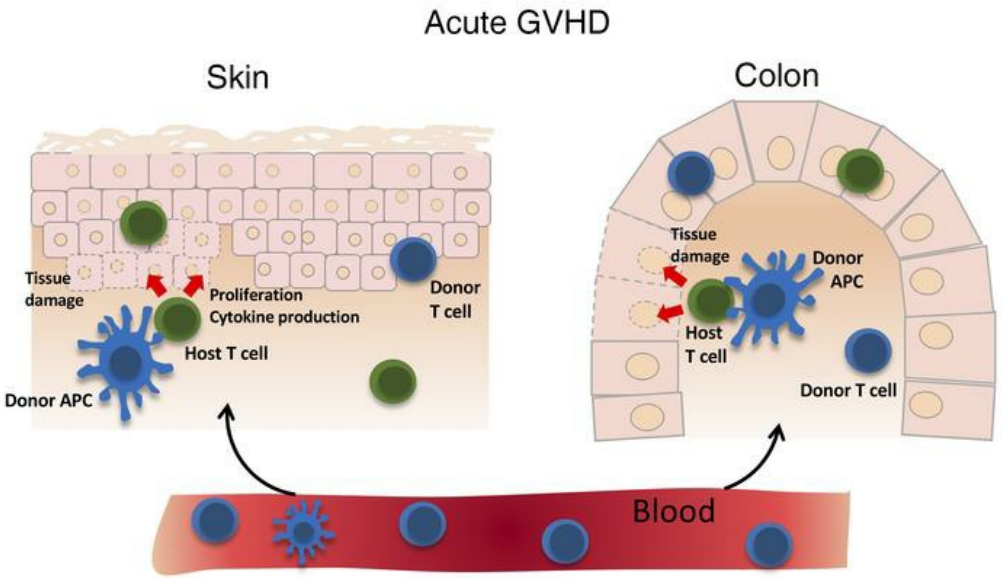

Peripheral host T cells survive hematopoietic stem cell transplantation and promote graft-versus-host disease

Sherrie J. Divito,[1] Anders T. Aasebø,[2] Tiago R. Matos,[1] Pei-Chen Hsieh,[1] Matthew Collin,[3] Christopher P. Elco,[4] John T. O'Malley,[1] Espen S. Bækkevold,[2] Henrik Reims,[5] Tobias Gedde-Dahl,[6] Michael Hagerstrom,[7] Jude Hilaire,[7] John W. Lian,[1] Edgar L. Milford,[8] Geraldine S. Pinkus,[7] Vincent T. Ho,[9] Robert J. Soiffer,[9] Haesook T. Kim,[10] Martin C. Mihm,[1] Jerome Ritz,[9] Indira Guleria,[8] Corey S. Cutler,[9] Rachael A. Clark,[1] Frode L. Jahnsen,[2] and Thomas S. Kupper[1]

[1]Department of Dermatology, Brigham and Women's Hospital, Boston, Massachusetts, USA. [2]Department of Pathology, University of Oslo and Oslo University Hospital–Rikshospitalet, Oslo, Norway. [3]Newcastle University, Translational and Clinical Research Institute, Newcastle upon Tyne, United Kingdom. [4]Department of Pathology and Laboratory Medicine, Brown University, Providence, Rhode Island, USA. [5]Department of Pathology, Oslo University Hospital–Rikshospitalet, Oslo, Norway. [6]Department of Hematology, Institute of Clinical Medicine, University of Oslo and Oslo University Hospital–Rikshospitalet, Oslo, Norway. [7]Department of Pathology and [8]Renal Transplant Program, Division of Renal Medicine, Brigham and Women's Hospital, Boston, Massachusetts, USA. [9]Division of Hematological Malignancies and Stem Cell Transplantation and [10]Department of Data Sciences, Dana-Farber Cancer Institute, Boston, Massachusetts, USA.

Graft-versus-host disease (GVHD) is a major cause of morbidity and mortality in hematopoietic stem cell transplantation (HSCT). Donor T cells are key mediators in pathogenesis, but a contribution from host T cells has not been explored, as conditioning regimens are believed to deplete host T cells. To evaluate a potential role for host T cells in GVHD, the origin of skin and blood T cells was assessed prospectively in patients after HSCT in the absence of GVHD. While blood contained primarily donor-derived T cells, most T cells in the skin were host derived. We next examined patient skin, colon, and blood during acute GVHD. Host T cells were present in all skin and colon acute GVHD specimens studied, yet were largely absent in blood. We observed acute skin GVHD in the presence of 100% host T cells. Analysis demonstrated that a subset of host T cells in peripheral tissues were proliferating (Ki67$^+$) and producing the proinflammatory cytokines IFN-γ and IL-17 in situ. Comparatively, the majority of antigen-presenting cells (APCs) in tissue in acute GVHD were donor derived, and donor-derived APCs were observed directly adjacent to host T cells. A humanized mouse model demonstrated that host skin-resident T cells could be activated by donor monocytes to generate a GVHD-like dermatitis. Thus, host tissue-resident T cells may play a previously unappreciated pathogenic role in acute GVHD.

Introduction

Graft-versus-host disease (GVHD) is a major cause of morbidity and mortality in hematopoietic stem cell transplantation (HSCT) (1–6). Current dogma holds that donor T cells, either transferred with or arising from the donor stem cell product, are activated in the setting of the inflammatory milieu generated by HSCT conditioning and mediate GVHD by damaging host tissues (reviewed in refs. 7, 8). Pretransplant conditioning regimens consist of one or more chemoimmunotherapeutic drugs, sometimes with total body irradiation, that are administered to patients before donor cell infusion. The goal is to reduce tumor load, provide physical space in host bone marrow to allow engraftment, and prevent host-mediated graft rejection by depleting host immune cells. Because host T cells in blood are depleted by conditioning regimens, it is assumed that host T cell immunity is abrogated. Therefore, the role of tissue-dwelling host T cells in human GVHD has not been investigated.

T cells were once thought to populate exclusively blood and secondary lymphoid organs at steady state. However, more recent observations suggest that the majority of memory T cells actually reside in human peripheral tissues, primarily in those in contact with the external environment: skin, gut, liver, and lung (9–13). Interestingly, these are the 4 tissues primarily affected by GVHD in human HSCT recipients. This novel population of tissue-resident T cells has been recognized as playing key roles in human health and disease (reviewed in refs. 14–16). Clinical observations suggest that skin-resident T cells survive "lymphocyte-depleting" chemotherapy, as patients who are profoundly lymphopenic following chemotherapy can still develop T cell–mediated drug rashes despite the absence of circulating lymphocytes. Skin biopsies from these patients demonstrate ample T cell infiltrates expressing markers consistent with tissue-resident memory T

▶ Related Commentary: p. 4532

Authorship note: SJD, ATA, and TRM share the first-author position. RAC, FLJ, and TSK share senior authorship.
Conflict of interest: JR receives research funding from Amgen, Equillium, and Kite/Gilead and serves on data safety monitoring committees for AvroBio and scientific advisory boards for Falcon Therapeutics, LifeVault Bio, Rheos Medicines, Talaris Therapeutics, and TScan Therapeutics. RJS serves on the board of directors for Kiadis and the Be The Match/National Marrow Donor Program, serves on the data safety monitoring board for Juno/Celgene, and has provided consulting for Gilead, Rheos Therapeutics, Cugene, Precision Bioscience, Mana Therapeutics, VOR Biopharma, and Novartis.

Submitted: May 8, 2019; **Accepted:** May 19, 2020; **Published:** July 27, 2020.
Reference information: *J Clin Invest*. 2020;130(9):4624–4636.
https://doi.org/10.1172/JCI129965.

cells (SJD, unpublished observations and ref. 17). Given the apparent durability of tissue-resident T cells, we hypothesized that host tissue-resident T cells survive HSCT conditioning and play a previously unappreciated role in GVHD.

Results

Skin host T cells survive HSCT. We collected skin and peripheral blood from 3 male patients receiving female donor HSC grafts to determine the origin of skin T cells after HSCT. Tissues were collected on the day of admission before the start of conditioning and again 30 ± 6 days after HSCT. Residual donor infusion product was also collected. Patients were conditioned with fludarabine (flu) + busulfan (bu); 2 received myeloablative dosing, and 1 received nonmyeloablative dosing (Supplemental Table 1; supplemental material available online with this article; https://doi.org/10.1172/JCI129965DS1). FFPE skin sections from post-HSCT samples were concurrently labeled via FISH for the X and Y chromosomes and via immunofluorescence (IF) for the T cell marker CD3 (Figure 1A). At 30 ± 6 days after HSCT, the majority of skin T cells in all 3 patients were host derived (Figure 1B) and appeared viable morphologically (Figure 1A). In contrast, host T cells composed the minority in peripheral blood after HSCT by short tandem repeat (STR) analysis (Figure 1B).

To determine whether T cells in skin after HSCT were host or donor derived, we performed high-throughput sequencing of the *TCRB* gene to identify clonal populations of memory T cells (18). Unique T cell clones were identified by their CDR3 sequences. In all 3 patients, the majority of T cell clones in skin after HSCT were identical to host skin T cell clones before HSCT (Figure 1C). The 20 most abundant T cell clones in host skin after HSCT and the comparable frequency of those clones in host skin before HSCT or donor infusion product, respectively, are shown in Figure 1D. Correlation between frequency of T cell clones in host skin before HSCT and skin after HSCT was high (r^2 patient 1-0.6464, patient 2-0.8740, patient 3-0.5867) (Supplemental Figure 1A). In contrast, higher frequency of clones in donor cells did not correlate with increased frequency in skin after HSCT (r^2 patient 1-0.0041, patient 2-0.0142, patient 3-0.0012) (Supplemental Figure 1, A and B). Of the top 100 most frequent clones in host skin after HSCT in each patient, only 0, 1, and 16, respectively, were donor derived (Supplemental Figure 1A). Thus, T cell clonality data paralleled the results from FISH-IF and STR analysis.

Host T cells are present in skin during acute GVHD. Given that skin T cells survived HSCT through 30 ± 6 days, a peak time point for onset of acute GVHD (19), and that the main tissues affected by GVHD are the same tissues containing large populations of tissue-resident T cells, we hypothesized that host T cells would be present in skin and gut during acute GVHD. Supplemental Table 2 details retrospective patient clinical data. Chemoimmunotherapeutics received by each patient before transplant are detailed in Supplemental Table 3 and Supplemental Table 4. Skin biopsies from 26 male patients with acute GVHD who received female donor transplants were labeled via FISH-IF to determine the number and percentage of host and donor T cells (Figure 2, A and B). Host T cells were observed in skin during acute GVHD of all patients studied, regardless of the conditioning regimen (myeloablative, median 39%, range 4%–100%) (nonmyeloablative, median 58%, range 3%–78%) ($P = 0.24$, Mann-Whitney U test, 2-tailed) (Figure 2B). Host T cells were observed throughout the skin, including within the epidermis and at the dermal-epidermal junction, the primary sites of damage in acute skin GVHD (Supplemental Figure 2).

We anticipated that the percentage of host T cells might decline with time after HSCT, as host T cells die off and/or as donor T cells accumulate in skin. We did not detect a statistically significant decrease in the percentage of host T cells in either the myeloablative or nonmyeloablative groups by linear regression (slope, −0.1384, $P = 0.09$; slope, 0.01133, $P = 0.94$, respectively), though there were a limited number of patients at late time points (Supplemental Figure 3A). There was no effect of patient age, GVHD prophylactic regimen, or type of donor transplant on percentage of host T cells in skin (Supplemental Figure 3, B–D).

To validate our FISH-IF results using a different approach, we used STR analysis on DNA from T cells extracted from an acute GVHD skin specimen (FFPE) via laser-capture microscopy. STR analytic data are shown for the most recently obtained patient skin specimen, as DNA is highly degraded in older FFPE samples and approximately 100 microns of tissue was necessary to perform the assay. In this sample, STR analysis demonstrated 25% host T cell chimerism in skin; this is compared with the 20% host T cells enumerated via FISH-IF in the same specimen (Supplemental Figure 4). This provides independent validation of the use of FISH-IF to quantify T cell chimerism.

To determine whether host T cells in skin included both $CD4^+$ and $CD8^+$ T cell subsets, representative patient skin sections were labeled via FISH-IF for CD3 and CD4. Multispectral microscopy/imaging software revealed the presence of both host $CD4^+CD3^+$ T cells and presumptive $CD4^-$ ($CD8^+$) $CD3^+$ T cells in skin specimens (Figure 2C). Though $CD4^-CD3^+$ cells could theoretically be γδ T cell type and negative for both CD4 and CD8, Norton et al., previously reported that γδ T cells constitute a small fraction (~4%) of T cells in skin during acute GVHD (20). We confirmed in a subset of our patients ($n = 5$) that the majority of T cells in skin during acute GVHD were αβ type, not γδ type, T cells (Supplemental Figure 5). Thus, our data demonstrate the presence of both $CD4^+$ and $CD8^+$ αβ TCR host T cells in acute GVHD skin lesions.

Given the discordance in T cell chimerism between skin and blood observed in our patients after HSCT, we compared T cell chimerism in skin and blood for patients diagnosed with acute GVHD. Seventeen of the 26 patients in the retrospective acute GVHD skin cohort had PBMCs collected at or near the time of acute skin GVHD. T cells were positively selected from PBMCs, purity was confirmed via flow cytometry (not shown), and T cell DNA was extracted and analyzed via STR analysis. Results demonstrated a clear population of residual host T cells in skin (determined via FISH-IF) despite the near or complete absence of host T cells in blood (determined by STR analysis) from paired specimens ($P < 0.001$, Wilcoxon's signed rank test, 2-tailed) (Figure 2D). This lack of concordance between skin and blood supports the findings from our prospective cohort study.

Host T cells are present in gut during acute GVHD. To assess host T cells in gut, a retrospective cohort study (Supplemental Table 2) of 15 male patients transplanted with female donor grafts who were diagnosed clinically and histopathologically with acute colonic GVHD

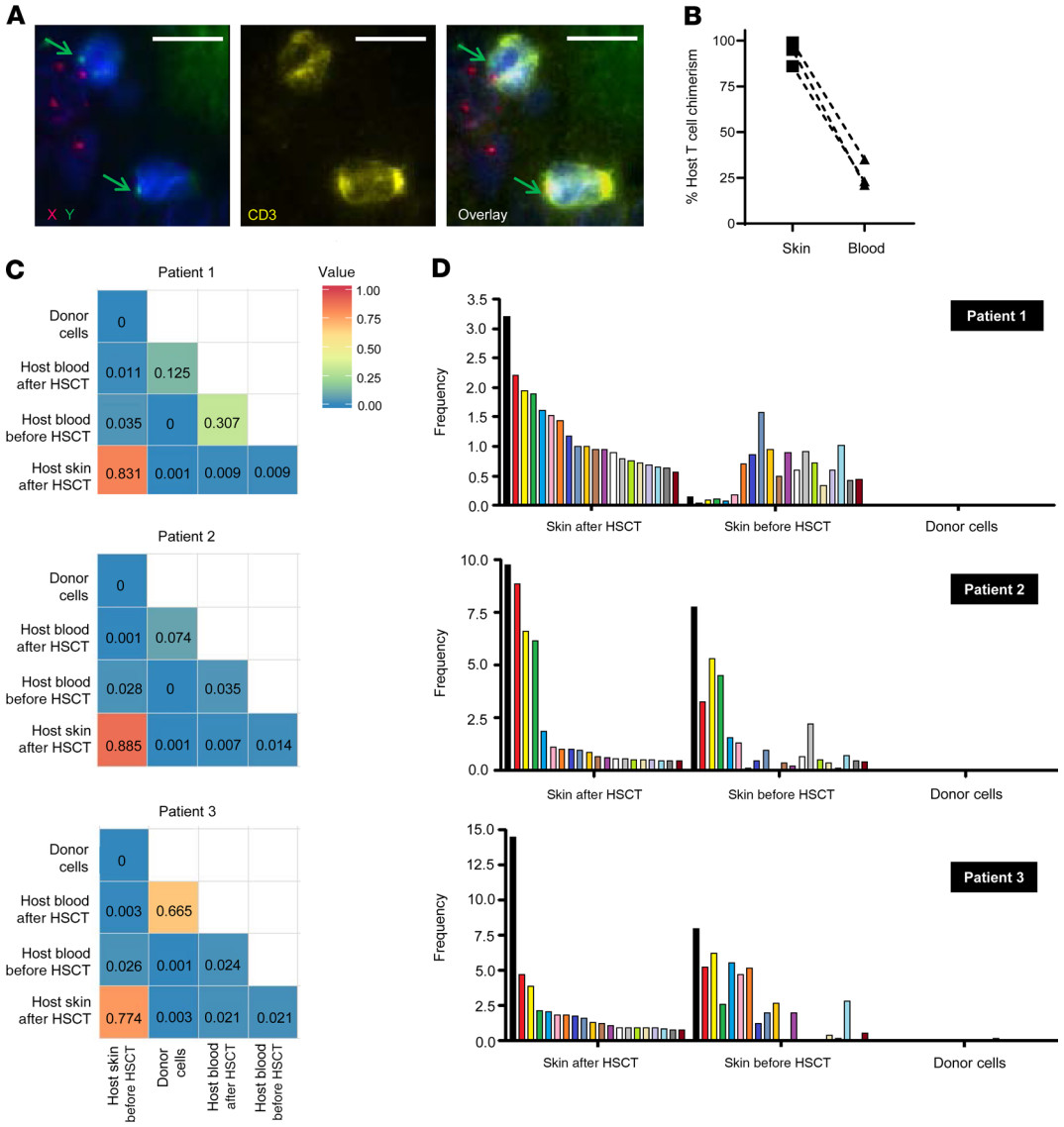

Figure 1. Host skin T cells survive HSCT conditioning. (**A**) Example of FISH-IF microscopy image of FFPE after HSCT skin showing the following: X chromosome, red; Y chromosome, green; CD3, yellow; DAPI nuclear stain, blue. Scale bars: 10 μm. Green arrows point to Y chromosomes in host T cells. (**B**) Percentage of host T cell chimerism in skin and blood in paired samples taken 30 ± 6 days after HSCT. Skin chimerism calculated via FISH-IF. Blood chimerism quantified via STR analysis. (**C**) Heatmap of Morisita overlap index for each patient. 0, no similarity; 1, complete similarity. (**D**) Bar graph for each patient showing the top 20 T cell clones in host skin after HSCT, whether those same clones were present, and if so, at what frequency, in donor cells (donor infusion product) or in host skin before HSCT. Each clone is color coded. (**A**–**D**) $n = 3$.

was performed. In this study, FISH-IF for both CD3 and CD8 revealed host $CD8^+CD3^+$ T cells and $CD8^-$ ($CD4^+$) $CD3^+$ T cells in the gut of all patients studied (Figure 3, A and B). Host T cells were present regardless of whether patients received myeloablative or nonmyeloablative conditioning (myeloablative, median 22%, range 6%–87%; nonmyeloablative, median 12%, range 7%–41%) ($P = 0.27$, Mann-Whitney U test, 2-tailed) (Figure 3B) and were present within both colon lamina propria and epithelium (Supplemental Figure 6, A and B). There were no significant differences in $CD8^+$ or $CD4^+$ T cell subsets between conditioning regimens (Supplemental Figure 6C).

The percentage of host T cells in acute gut GVHD specimens did not show a statistically significant decrease with time, combining myeloablative and nonmyeloablative groups (linear regression, slope, –0.10, $P = 0.54$), though again there were a limited number of patients at later time points (Supplemental Figure 7A). As was the case in skin, host T cell chimerism in gut significantly diverged from peripheral blood (Wilcoxon's signed rank test, 2-tailed, $P = 0.01$) (Figure 3C). There was no association observed between the percentage of host T cells and age at time of transplant or type of donor transplant (Supplemental Figure 7, B and C).

Host T cell chimerism in skin is affected by acute GVHD. To further elucidate the impact of time and acute GVHD on host T cell chimerism in peripheral tissue, skin was sampled in an additional prospective patient cohort (referred to as UK cohort). Supplemental Table 5 details UK-cohort clinical data, which was originally described previously (21). In this prospective cohort, skin samples were collected for T cell analysis from 34 patients at 40, 100, and/or 365 days after transplant (8 patients were biopsied at 2 time

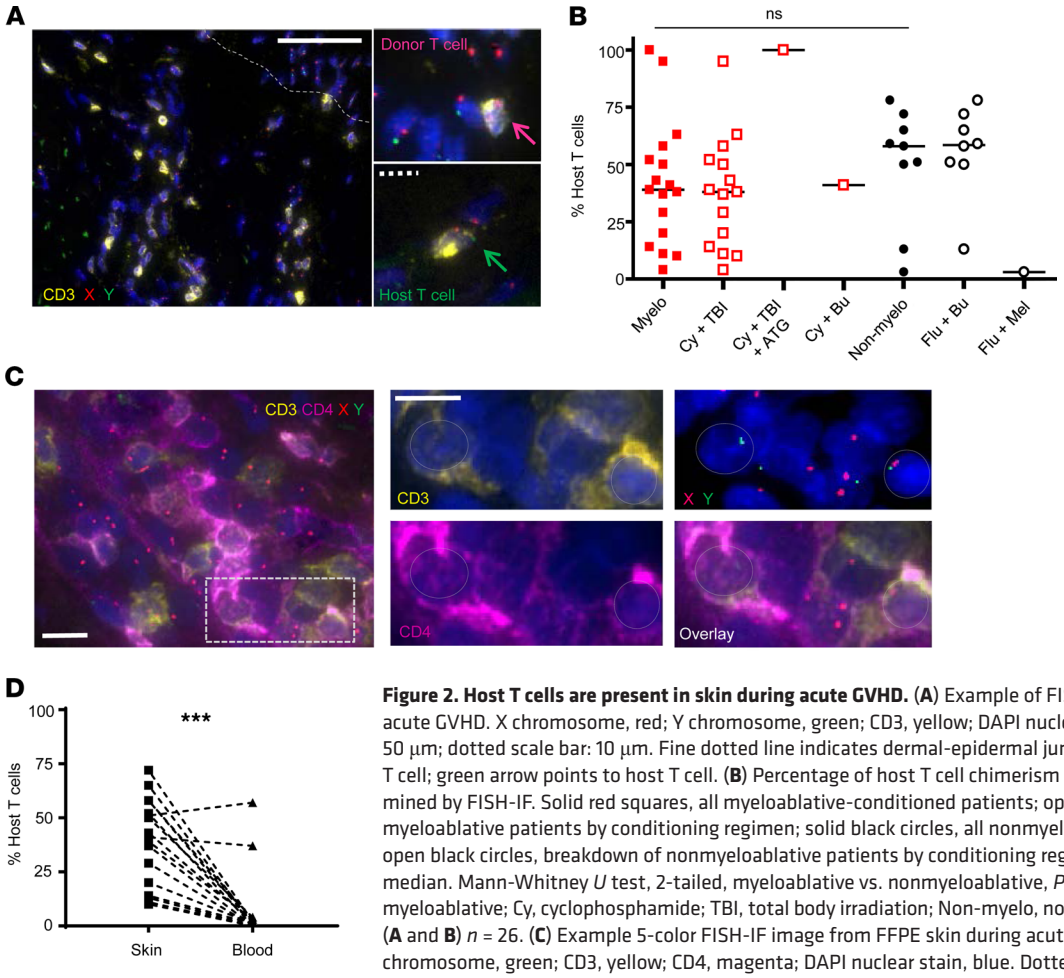

Figure 2. Host T cells are present in skin during acute GVHD. (**A**) Example of FISH-IF from FFPE skin during acute GVHD. X chromosome, red; Y chromosome, green; CD3, yellow; DAPI nuclear stain, blue. Solid scale bar: 50 μm; dotted scale bar: 10 μm. Fine dotted line indicates dermal-epidermal junction. Pink arrow points to donor T cell; green arrow points to host T cell. (**B**) Percentage of host T cell chimerism in skin during acute GVHD, determined by FISH-IF. Solid red squares, all myeloablative-conditioned patients; open red squares, breakdown of myeloablative patients by conditioning regimen; solid black circles, all nonmyeloablative-conditioned patients; open black circles, breakdown of nonmyeloablative patients by conditioning regimen. Black lines indicate median. Mann-Whitney *U* test, 2-tailed, myeloablative vs. nonmyeloablative, $P = 0.24$, not significant. Myelo, myeloablative; Cy, cyclophosphamide; TBI, total body irradiation; Non-myelo, non-myeloablative; Mel, melphalan. (**A** and **B**) $n = 26$. (**C**) Example 5-color FISH-IF image from FFPE skin during acute GVHD. X chromosome, red; Y chromosome, green; CD3, yellow; CD4, magenta; DAPI nuclear stain, blue. Dotted white rectangle outlines region of enlarged images. Scale bars: 10 μm. Dotted gray circles outline $CD3^+CD4^+$ host T cells. $n = 5$. (**D**) Percentage of host T cell chimerism in skin, determined by FISH-IF, and blood, determined by STR analysis, at the time of acute GVHD. $n = 17$. Broken lines indicate paired specimens. Wilcoxon's signed rank test, 2-tailed. $^{***}P < 0.001$.

points, and 3 patients were biopsied at all 3 time points). Samples were categorized by whether each patient had no acute skin GVHD, active acute skin GVHD, or history of acute skin GVHD that was resolved at time of biopsy. Active acute skin GVHD was further divided into new-onset acute skin GVHD at time of biopsy or acute skin GVHD at time of biopsy plus prior episode of acute skin GVHD (Figure 4, A and B). Chimerism was quantified by sequential FISH-IF performed on cytospins of migratory cells (Figure 4C). Similarly to above observations, data from this cohort demonstrate that in the absence of acute skin GVHD, host T cells comprised the majority of T cells in skin through 1 year after transplant (40 days, $n = 6$, median 97%, range 69%–100%; 100 days, $n = 12$, median 69%, range 7%–100%; 365 days, $n = 1$, 56%) (Figure 4, A and B). Though there was a small decrease in median percentage of host T cells with time, this was not statistically significant ($P > 0.05$, Dunn's multiple comparison's test, 40 vs. 100 days). Moreover, skin samples from new-onset active acute GVHD likewise contained substantial host T cell populations (40 days, $n = 4$, median 79%, range 39%–93%; 100 days, $n = 1$, 28%) (Figure 4, A and B). This parallels findings from the above retrospective cohorts and supports that the proportion of host versus donor T cells may not be a critical factor in the development of acute GVHD.

Interestingly, dividing active acute GVHD into new-onset acute disease versus active disease in a patient with history of acute skin GVHD revealed that a prior history of acute skin GVHD was overall associated with reduced host T cell chimerism in skin (Figure 4, A and B). In keeping with this observation, median host T cell chimerism was also low in skin of patients who previously had acute GVHD (i.e., biopsy taken after GVHD resolution). This finding was not universal though, as some patients retained substantial percentages of host T cells despite history of acute GVHD (Figure 4, A and B). These data suggest that acute GVHD (or its treatment) may preferentially eliminate host T cells from skin, but that in some cases, stable mixed chimerism can occur.

Host T cells are activated in acute GVHD. One patient from the retrospective cohort demonstrated 100% host T cells in skin (i.e., donor T cells could not be identified) and another patient 95% host T cells in skin during acute GVHD. Both patients had stage 1 skin disease. An additional patient demonstrated 100% host T cells in skin during acute GVHD; however, he was excluded from the study because there was insufficient biopsy material available for further analysis (not shown). The cohort patient with 100% host T cells received anti-thymocyte globulin (ATG)

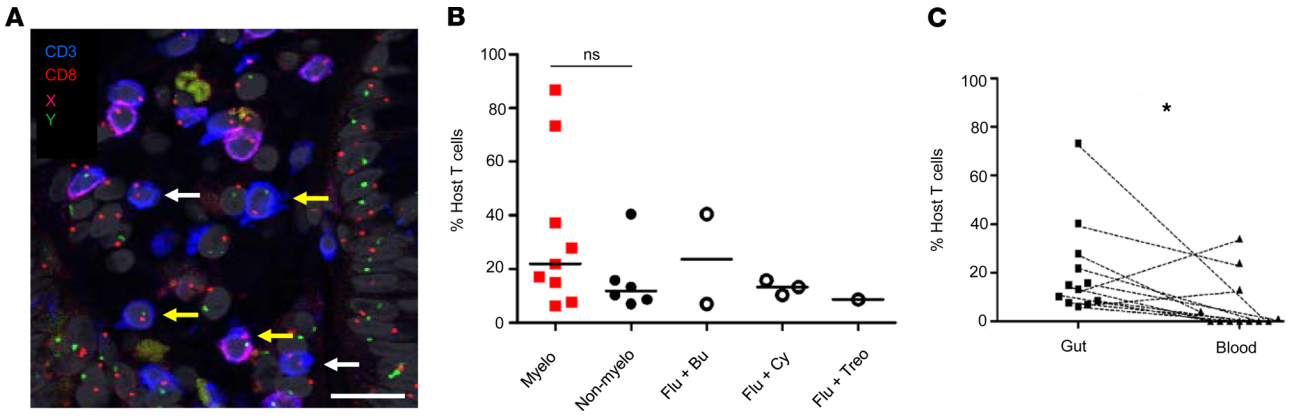

Figure 3. Host T cells are present in gut during acute GVHD. (**A**) Example of FISH-IF from FFPE colon during acute GVHD. X chromosome, red; Y chromosome, green; CD3, blue; CD8, red; Hoechst nuclear stain, gray. Scale bar: 20 μm. Blue staining indicates $CD4^+$ T cells ($CD3^+CD8^-$), whereas pink staining (mixed blue and red) indicates $CD3^+CD8^+$ T cells. White arrows point to donor (XX) T cells; yellow arrows point to recipient (XY) T cells. (**B**) Percentage of host gut T cell chimerism in acute GVHD. Red squares, myeloablative-conditioned patients; solid black circles, nonmyeloablative-conditioned patients; open black circles, breakdown of nonmyeloablative conditioning regimens. Black lines indicate median. Mann-Whitney *U* test, 2-tailed, myeloablative vs. nonmyeloablative, $P = 0.27$, not significant. Treo, treosulfan. (**A** and **B**) $n = 15$. (**C**) Percentage of host gut T cell chimerism determined by FISH-IF versus peripheral blood chimerism determined by STR analysis. $n = 12$. Broken lines indicate paired samples. Wilcoxon's signed rank test, 2-tailed. $^*P = 0.01$.

as part of his conditioning regimen. ATG would be expected to deplete all circulating (donor plus host) T cells (22), but it appears that noncirculating tissue-resident host T cells were spared. There is precedent that depleting antibody therapies deplete circulating but not skin-resident T cells (23).

Figure 5A illustrates the degree of tissue damage observed in the patient with 100% host T cells in skin during acute GVHD. Immunofluorescent staining demonstrated that a subset of host $CD3^+$ T cells in skin in this patient were in cell cycle ($Ki67^+$) (Figure 5B) and that a subset of $CD3^+$ T cells expressed the proinflammatory cytokines IFN-γ and IL-17 in situ (Figure 5C). There were no detectable $Foxp3^+$ T cells (regulatory T cell marker) or IL-10–producing (an immunoregulatory cytokine) T cells observed in this patient's skin (not shown).

We could not reliably perform IF staining for cytokines in conjunction with FISH labeling due to technical limitations. However, because Ki67 is expressed only in activated T cells that have entered the cell cycle, FISH-IF for Ki67 and CD3 was performed in gut GVHD samples as a surrogate for activation. Importantly, a lack of Ki67 does not mean that a T cell is not activated, as activated memory T cells may remain in G_0 (24). Ki67 was expressed by host $CD3^+$ T cells in colon specimens in 12 of 15 patients, with a median of 5% (range 0-30%) (Figure 5D). Cumulatively, these data suggest that at least a subset of host T cells are activated and contribute to the inflammatory milieu during acute GVHD.

Finally, there was no statistically significant association between the percentage of host or donor T cells and clinical or histological disease severity in skin (Kruskal-Wallis, $P = 0.39$ and $P = 0.51$, respectively) or in gut (Kruskal-Wallis, $P = 0.34$ and $P = 0.38$, respectively) (Figure 5E), suggesting that the proportion of host and donor T cells in skin or gut per se is not a key determinant for acute GVHD severity.

Donor APCs infiltrate peripheral tissue in high numbers during acute GVHD. These data raise the question of how host T cells could become activated in peripheral tissues after HSCT. The accompanying paper by Jardine et al., demonstrates that donor monocyte-derived macrophages infiltrate skin during acute GVHD in high numbers and, at least ex vivo, are capable of presenting antigen to and stimulating allogeneic T cells (25). In concordance, we observed by FISH-IF that the majority of $HLA\text{-}DR^+$ (class II^+) $CD3^-$ antigen-presenting cells (APCs) were of donor origin (Y negative) (median 92%, range 76%–100%) ($P = 0.004$ compared with T cells, Wilcoxon's signed rank test, 2-tailed) in the gut during acute GVHD and could be found adjacent to host (Y positive) $CD3^+$ T cells (Supplemental Figure 8, A and B).

Donor monocytes with host skin resident T cells induce a GVHD-like dermatitis in the absence of donor T cells. Based on these findings, we used a human-engrafted mouse model to test the ability of host skin T cells to mediate GVHD in the absence of donor T cells. NSG mice were grafted with healthy adult human skin, which contains abundant memory T cells ("host"). These grafted mice were then subsequently adoptively transferred with "donor" (i) allogeneic CD25-depleted PBMCs (to deplete donor regulatory T cells), (ii) allogeneic positively selected monocytes, or (iii) saline (Figure 6A). Adoptively transferred PBMCs contained donor T cells, whereas mice injected with monocytes were devoid of donor T cells. Adult human skin has been estimated as containing roughly 1 million memory T cells/cm^2, the majority of which are nonrecirculating resident memory T cells (12, 26). Therefore, the only T cells in monocyte-infused mice were those derived from the host adult skin graft. Grafts were harvested 3 weeks after donor cell infusion and analyzed by histology, quantitative real-time PCR (RT-PCR), and high-throughput TCR sequencing (HTS).

A GVHD-like dermatitis developed in skin grafts; this was characterized by acanthosis, parakeratosis, basal layer vacuolization, keratinocyte dyskeratosis, lymphocyte exocytosis into the epidermis, and dermal lymphocytic infiltration (Figure 6, B–D). Remarkably, histopathological findings were similar between skin grafts in mice injected with PBMCs versus monocytes alone. Severity, as determined via histologic grading, was mildly but not significantly reduced in the absence of infused donor T cells (monocyte-infused group) (Figure 6E).

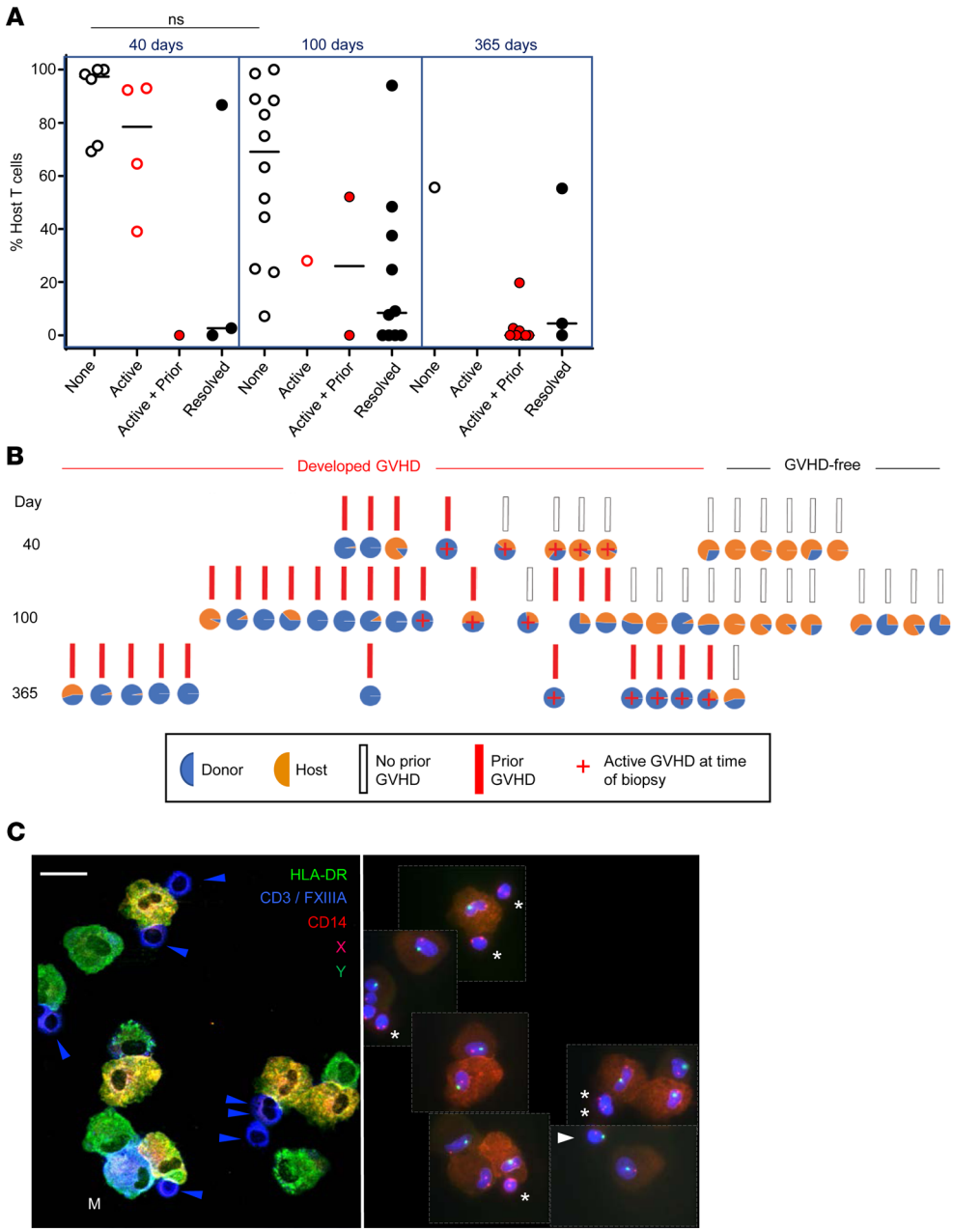

Figure 4. Acute GVHD affects host T cell chimerism in skin. (**A**) Percentage of host T cell chimerism as quantified by sequential FISH-IF on cytospins of skin migratory cells at 40, 100, and 365 days after transplant. Open black circles, no GVHD; open red circles, active acute skin GVHD at time of biopsy; closed red circles, active acute skin GVHD and prior history of active acute skin GVHD; closed black circles, history of acute skin GVHD resolved at time of biopsy. Black lines indicate median. Dunn's multiple comparison's test for no GVHD 40 vs. 100 days. $P > 0.05$, not significant. (**B**) FISH-IF data for individual patients depicted in pie charts (gold, host; blue, donor) at 40, 100, and/or 365 days after transplant. Red plus sign indicates active acute skin GVHD at time of biopsy. Red bars indicate prior history of acute skin GVHD. Open bars indicate no prior history of acute skin GVHD. (**C**) Representative FISH-IF of a female patient transplanted with a male donor, skin sample taken at 40 days after transplant. This patient had a prior history of acute skin GVHD resolved at time of biopsy. Staining was performed as follows: HLA-DR, green; CD14, red; CD3 and factor XIIIA, both blue (easily discernible by morphology); FISH, X chromosomes, pink; Y chromosomes, green. Montages of corresponding FISH images are outlined with gray dotted squares. Quantification yielded host T cell chimerism of 87% and myeloid cell ($HLA\text{-}DR^+CD14^+$) chimerism of 98% donor. Asterisks, host (XX) T cells; white arrowhead, donor (XY) T cell; blue arrowheads, $CD3^+$ T cells; M, macrophage. Scale bar: 20 μm. (**A**–**C**) $n = 34$.

T cell numbers in the skin grafts of monocyte- and PBMC-injected mice were not significantly different, as assessed by quantitative RT-PCR for *CD3E* gene expression (Figure 6F) and HTS of the *TCRB* gene (Figure 6G). *TNFA*, *IL-9*, *IL-17A*, and *IL-22* levels in the skin graft, assessed by quantitative RT-PCR, were also similar in monocyte- and PBMC-injected mice (Supplemental Figure 9, A–D). *IFNG* was the only cytokine significantly increased in PBMC-injected versus monocyte-injected mice (Supplemental Figure 9E).

We next studied skin grafts by HTS of the *TCRB* gene to determine whether host skin-resident T cell clones proliferated and expanded in situ in the skin after encounters with donor monocytes. We identified skin-resident T cell clones by CDR3 sequences that were present in both saline-injected and monocyte-injected mice grafted with skin from the same donor. We measured the frequency of these common clones in saline- versus monocyte-injected mice to determine cell proliferation. The frequency of host skin-resident T cell clones was increased in the skin grafts of monocyte-injected mice, suggesting local proliferation and expansion within the skin (Figure 6H). Parallel analyses of PBMC-injected mice also showed host skin T cell expansion, but this was not significantly different between monocyte-injected and PBMC-injected mice (Figure 6I).

To confirm that host skin T cells were responsible for the GVHD-like dermatitis observed in monocyte-injected mice, we grafted mice with human foreskin, a tissue that contains APCs, but few if any resident memory T cells (24). Foreskin-grafted mice were injected i.v. with allogeneic monocytes alone or with CD25-depleted PBMCs. Mice injected with PBMCs developed a robust GVHD-like dermatitis. In contrast, monocyte-injected mice bearing skin grafts that lacked host T cells did not develop

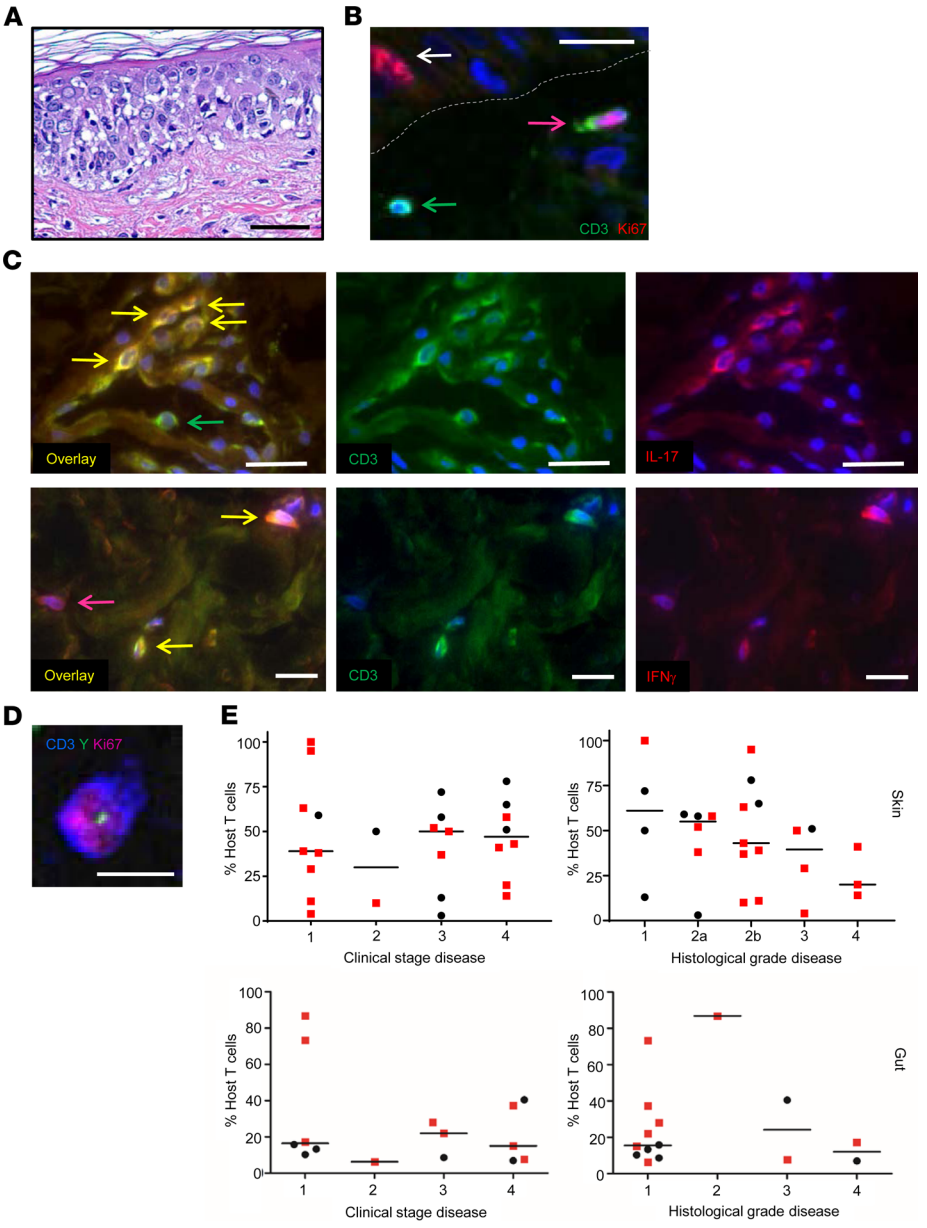

Figure 5. Host T cells in skin and gut during acute GVHD are activated. (**A**) Example of H&E staining of skin from patient with 100% host T cells. Scale bar: 50 μm. (**B**) Example of IF staining from the same patient, as follows: CD3, green; Ki67, red; DAPI nuclear stain, blue. Gray dotted line shows dermal-epidermal junction. Pink arrow points to $Ki67^+CD3^+$ T cell; green arrow points to $Ki67^-CD3^+$ T cell; white arrow points to $Ki67^+$ keratinocyte. Scale bar: 20 μm. (**C**) Example of IF staining of the same patient, as follows: CD3, green; proinflammatory cytokines, IFN-γ or IL-17, red; DAPI nuclear stain, blue. Scale bars: 20 μm. Yellow arrows point to cytokine-producing $CD3^+$ T cells; green arrow points to $IL\text{-}17^-CD3^+$ T cell; pink arrow points to $IFN\text{-}\gamma^+CD3^-$ cell. (**D**) Example of FISH-IF staining as follows: Y chromosome, green; CD3, blue; Ki67, magenta; Hoechst nuclear stain, gray. Scale bar: 20 μm. $n = 15$. (**E**) Percentage of host T cells in skin during acute GVHD versus clinical stage disease (left) and histologic grade (right). Skin, top row, $n = 26$; gut, bottom row, $n = 15$. Red squares, myeloablative-conditioned patients; black circles, nonmyeloablative-conditioned patients. Black lines indicate median. Kruskal-Wallis test, skin and gut clinical stage and histological grade, not significant.

inflammation (Figure 6J), indicating that the dermatitis observed in adult skin-grafted mice was mediated by host skin-resident T cells.

Discussion

It has long been presumed that T cell chimerism in blood and bone marrow reflects T cell chimerism in all peripheral tissues, based on the assumption that conditioning regimens deplete host T cells in blood, bone marrow, and peripheral tissues equally. The appreciation that memory T cells are abundant in human peripheral tissues, however, is relatively recent (ref. 11 and reviewed in refs. 14–16). In our studies, host T cell chimerism in skin and gut diverged markedly from host T cell chimerism in blood, indicating that T cells resident in peripheral tissues are highly resistant to depletion, even after high-intensity conditioning. Therefore, an important finding of this study is that T cell chimerism in blood and/or bone marrow does not reflect, and should not be used to assess, chimerism in peripheral tissues. This is notable because T cells are more abundant in peripheral tissues than in circulation (26).

Given that skin-resident T cells appear to survive HSCT conditioning and that the tissues known to contain large numbers of resident T cells are the main target organs in GVHD, we hypothesized that host T cells would be present in target tissues during acute GVHD. Using 2 retrospective cohorts totaling 41 patients across 2 countries and a prospective cohort of 34 patients from a third country, we observed host T cells in skin and colon during acute GVHD. While this study could not determine with certainty the origin of the host T cells (tissue resident vs. migratory), the efficacy of conditioning regimens at depleting circulating T cells strongly suggests that the surviving host T cells were predominantly resident in tissue in situ. A prospective study tracking T cell clones from before HSCT through the post-HSCT period and during acute GVHD will be necessary to address this.

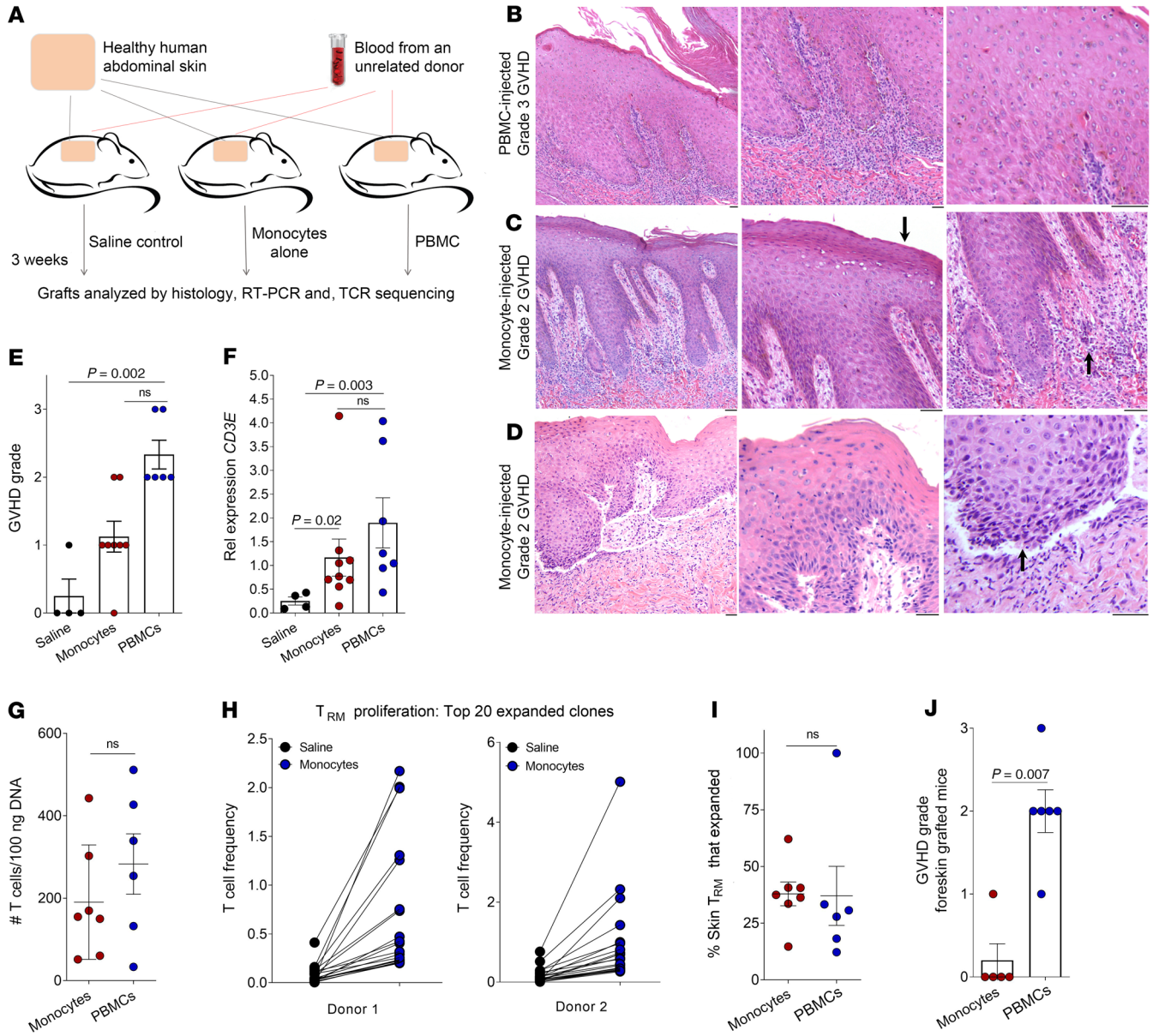

Figure 6. Host skin T cells induce GVHD-like dermatitis independently of donor T cells in human skin–grafted mice. (**A**) NSG mice were grafted with human skin and i.v. injected with saline, allogeneic monocytes alone, or allogeneic CD25-depleted PBMCs (labeled as PBMCs); skin grafts were studied after 3 weeks. (**B**) Mice injected with PBMCs developed a GVHD-like dermatitis characterized by acanthosis, parakeratosis, dyskeratosis, and lymphocytic infiltrates. (**C**) Monocyte-injected mice developed similar changes, including lymphocytic infiltrates (left panel), epidermal acanthosis and parakeratosis (middle panel), and basal layer vacuolization and destruction of rete ridges (right panel). (**D**) A second skin/blood pair with similar changes is shown. (**B**–**D**) Scale bars: 50 μm. (**E**) Histologic grading of GVHD-like dermatitis in skin grafts of monocyte- and PBMC-injected mice. (**F** and **G**) T cell numbers in skin, assessed by *CD3E* gene expression (**F**) and by HTS (**G**), were similar in monocyte- and PBMC-injected mice. (**H**) Host skin-resident T cells (T_{RM}) proliferate after exposure to donor monocytes. The frequencies of the 20 most frequent T cell clones found in grafts from both saline- and monocyte-injected mice are shown. (**I**) Similar percentages of T_{RM} clones proliferated in monocyte- and PBMC-injected mice. Histology and transcript analysis performed on saline-injected (n = 4), monocyte-injected (n = 9), and PBMC-injected (n = 7) mice. Clonality performed on monocyte-injected (n = 7) and PBMC-injected (n = 6) mice. (**J**) GVHD did not develop in the absence of host skin T cells. Mice grafted with human foreskin, which contains APC, but lacks T cells, and infused with PBMCs (n = 6) developed GVHD-like dermatitis, but monocyte-injected (n = 5) mice did not. Mean and SEM (error bars) are shown. Differences between 2 independent groups were detected using Mann-Whitney *U* test, 1-tailed. One-way Kruskal-Wallis test with Dunn's post test was used for comparing multiple independent groups.

Our data support previous findings that T cells in peripheral tissues during acute GVHD bear αβ TCRs rather than γδ TCRs (20, 27). Attempts at staining for NKT cells or mucosal-associated invariant T cells (which could be phenotypically $CD3^+CD4^-CD8^-$) using antibodies for Vα24-Jα18 and Vα7.2, respectively, were unsuccessful in our FFPE samples. Thorough analysis of these populations using flow cytometry performed on freshly collected tissue would be technically challenging, but potentially interesting, given findings that suggest invariant NKT cells may play a regulatory role in GVHD (28).

Korngold and Sprent showed 40 years ago that donor T cells responding to host alloantigen are required for GVHD in a mouse

model (29). Nearly all subsequent mouse models of GVHD have been engineered under the assumption that donor T cells are both necessary and sufficient for acute GVHD. A review of the literature showed that 2 GVHD mouse studies, using naive donor to naive recipient, investigated host T cells in lymphoid tissues that survived conditioning. These data suggested a possible regulatory role for host T cells against chronic GVHD (30) and donor lymphocyte infusion–associated GVHD (31). Our data support a proinflammatory role for host T cells in peripheral tissues, though our study focused on acute rather than chronic GVHD and only 1 patient had received donor lymphocyte infusion. Notably, GVHD mouse models nearly always employ naive donor and recipient mice housed in specific pathogen–free conditions. Importantly, these mice typically lack the robust and diverse memory T cell population, in particular tissue-resident memory T cells, that are present in humans (32) and that may be key contributors to skin and gut GVHD.

The observation that a subset of host T cells in peripheral tissues were proliferating indicates that they were activated and not quiescent. This is consistent with the observations from the human engrafted mouse experiments, where host T cells were shown to have expanded through proliferation by molecular assessment of *CD3E* mRNA and *TCRB* DNA. Host T cells could clearly mediate a GVHD-like process in our human-engrafted mouse model, as host skin T cells and positively selected donor monocytes were sufficient to induce a GVHD-like dermatitis. Histopathologic severity in the donor monocyte–only injected mice was slightly, but not significantly, reduced compared with that in the mice that received donor T cells (CD25-depleted PBMC-injected mice). Grafts with skin-resident T cells from mice injected with donor monocytes, but not donor T cells, contained *IL-17*, *IL-22*, and *TNFA* comparable to that of mice receiving donor T cells, suggesting that production of these cytokines was due to host skin-resident T cells. The addition of donor T cells to the humanized mouse model resulted in significantly increased *IFNG* within grafts ($P = 0.02$), suggesting that Th1 polarization may be responsible for the increased disease severity observed in mice receiving donor T cells.

The observation that 1 patient manifested 100% host T cell chimerism and another patient 95% host T cell chimerism in skin during acute GVHD supports the idea that host T cells may be sufficient for what was clinically and histopathologically diagnosed as GVHD and that the (near complete) absence of donor T cells may result in a milder form of GVHD. Interestingly, depletion of $CD45RA^+$ naive T cells from allogeneic grafts before transplantation does not reduce the incidence of acute GVHD, but does reduce disease severity (33), supporting our observations. It is seemingly plausible that, while both donor and host T cells may be required for severe acute GVHD, host T cells alone may be sufficient for less florid GVHD. Whether host T cell activation synergizes with donor T cell activation to generate a more severe phenotype cannot be determined from these experiments.

This prompts the question of whether donor and host T cells can coexist. Intriguingly, it may be the attempt of host and donor T cells to eliminate each other that is part and parcel of GVHD. To this point, Figure 4A shows that the percentage of host T cells in skin is reduced in patients with prior/resolved GVHD, suggesting that acute GVHD (or its treatment) may preferentially eliminate host T cells from skin. However, there were multiple cases in this same cohort where substantial host T cell populations remained despite prior/resolved acute GVHD, supporting that stable mixed chimerism is possible in peripheral tissues despite GVHD. Stable mixed chimerism in circulating T cell populations after stem cell transplantation has been previously reported by multiple groups, indicating the possibility of mutual "tolerance" (34–37). The same appears to be true in peripheral tissues as well in the setting of solid organ transplantation (38, 39).

Residual host T cells in circulation/lymphoid organs are a risk factor for graft rejection (40–42), though residual host T cells in peripheral tissues in relation to graft rejection have not been studied. None of the patients in our cohorts had graft rejection. Given the marked divergence in T cell chimerism between peripheral tissues (skin/gut) and blood observed in this study, we would hypothesize that graft rejection would more likely align with residual T cell populations in circulation and bone marrow/lymphoid organs rather than host T cell populations in peripheral tissues. However, we cannot draw any definitive conclusions from our data, and this is an area of investigation to be pursued.

The effect of T cell depletion on GVHD is an important issue, as it is commonly presumed that T cell depletion abrogates GVHD and therefore donor T cells are necessary and host T cells insufficient for disease. However, even with complete T cell depletion from donor grafts, the reduction in acute GVHD incidence is highly variable across studies and is not absolute (reviewed in ref. 43). Whether the variable results are due to incomplete donor T cell depletion or to residual host T cells is unclear. Further, studies often report a reduction in grade II–IV disease, but do not comment on incidence of mild GVHD, where host T cells may be prominently involved. Most importantly, commonly used T cell–depletion strategies have significant off-target effects. For example, alemtuzumab may deplete and/or reduce functionality of monocytes and monocyte-derived APCs in addition to T cells (44, 45). Based on our data, donor monocytes may be critical in stimulating host T cell–mediated GVHD. ATG likewise targets numerous cell populations, including APCs (46). Even in a study using anti-CD2 and anti-CD3 antibodies, which would be expected to target only T cells (and potentially NKT cells), an effect on the myeloid compartment was reported by investigators (47). Further studies are clearly needed to delineate a potential role for host T cells in GVHD in T cell–depleted grafts.

These data also raise the question of GVHD incidence and severity in patients transplanted for severe combined immunodeficiency (SCID), a rare genetic disease affecting T (and potentially B and NK) cell development or function (48). SCID patients can develop GVHD (48–52). Though this might suggest that donor T cells alone are sufficient for GVHD, several factors complicate interpretation of this observation. First, GVHD data are quite sparse in SCID patients due to the rarity of disease and to the variability in conditioning, donor stem cell source, and GVHD prophylaxis used in each patient (48–50, 52). Moreover, the SCID phenotype is quite heterogeneous, as it is caused by mutations in several different genes; in fact, some SCID patients have circulating T cells (48). The question of whether these patients also have tissue-resident T cells has not been addressed, to our knowledge. Interestingly, there are reports of SCID patients receiving T cell–depleted donor stem cells, yet developing GVHD (50, 52). Whether these

patients had functional host T cells in tissue or developed GVHD from incomplete donor T cell depletion is unclear. Deeper interrogation of GVHD in SCID patients may yield valuable insight into the relative contributions of donor and host T cells to disease.

There are several potential mechanisms by which host T cells might become activated even in a fully MHC-matched allogeneic transplant. Donor or host APCs expressing self-MHC could present minor-mismatched alloantigen to T cells. Host APCs could present neoantigens expressed in the setting of conditioning-induced tissue damage that would be viewed by T cells as foreign or self-peptides with loss of T cell tolerance in the setting of robust inflammation. Finally, antigen-independent bystander activation of T cells via cytokine stimulation could occur. Haniffa et al. evaluated chimerism of different skin APC populations following HSCT. Dermal dendritic cells had high turnover and Langerhans cells intermediate turnover, while host resident macrophages persisted long term in skin after transplant in the absence of GVHD (21). The accompanying paper by Jardine et al. illuminates that donor $CD11c^+CD14^+$ monocyte–derived macrophages are the predominant APC population in skin during active acute GVHD and that these APCs are capable of activating allogeneic T cells ex vivo (25). We similarly observed donor APC-infiltrating gut in high percentages during acute GVHD, supporting the possibility of donor APC/host T cell interaction. The human-engrafted mouse model demonstrated that the combined presence of host skin T cells and donor monocytes induced GVHD-like dermatitis, but the absence of either cell population prevented disease. Whatever the mechanism, our observations suggest the term *graft-versus-host disease* does not fully describe the pathophysiology, as host-versus-graft events appear to contribute to the clinical and histopathological appearance of this disease. Importantly, these data do not in any way argue against the role of donor T cells in GVHD.

This study reveals what we believe to be a novel avenue of research into the pathophysiology of GVHD. The limitations of this study include the small sample sizes and the retrospective nature of the human acute GVHD studies necessitating use of FFPE specimens. Archival FFPE tissue is more challenging to stain via IF (due to crosslinking of epitopes by formalin) and can suffer from DNA degradation, thus hampering FISH. More extensive analysis of host T cells in patient samples was therefore precluded. Moving forward, a large prospective human study in which fresh tissue is collected will allow for deeper interrogation of host T cell phenotype and function. Coupled with humanized mouse models, such studies will be able to evaluate the true contribution of host T cells to acute GVHD. Though challenging, these studies should be pursued, given the possible important implications for clinical care.

Methods

Patients. For the prospective study, USA cohort, adult males undergoing a first allogeneic HSCT receiving female donor grafts were enrolled. Subjects with underlying T cell malignancies or HIV were excluded. Skin biopsy and peripheral blood were collected on the day of admission for transplantation before conditioning and again 30 ± 6 days after HSCT. Additionally, residual donor cells from the stem cell product bag were collected.

For the prospective study, UK cohort, adult females undergoing a first allogeneic HSCT receiving male donor grafts were enrolled. Skin biopsies were collected at 40, 100, and/or 365 days after transplant.

For retrospective studies, sections were obtained from FFPE skin (Brigham and Women's Hospital/Dana-Farber Cancer Institute) or colonic (Oslo University Hospital) biopsies previously acquired for clinical purposes from adult male patients transplanted from female donors. Because biopsies were collected for clinical purposes, they were obtained at variable time points after disease onset, so in some cases, they were collected after initiation of systemic immunosuppression. Medical record review confirmed that each patient was diagnosed clinically with acute skin or gut GVHD, and each patient's tissue biopsy was read by an experienced pathologist as consistent with GVHD. Samples were excluded from any patient with underlying T cell malignancy or history of prior transplant or from patients with limited available tissue sample. PBMCs taken during the same episode of acute GVHD were available for analysis for some patients.

For simplicity, reduced intensity and nonmyeloablative conditioning regimens have been combined and are referred to as "nonmyeloablative" conditioning to distinguish them from myeloablative conditioning.

T cell selection from PBMCs and flow cytometry. For the skin cohort, T cells were positively selected from PBMCs using the Human CD3 Positive Selection Kit (Stem Cell Technologies). Percentage selection was confirmed by staining for CD2 (RPA-2.10, 300213, BioLegend) and analysis on a FACSCanto flow cytometer (BD Biosciences).

High-throughput TCRB sequencing. DNA was extracted from approximately 80–100 microns of OCT-embedded frozen skin specimens using the QIAamp DNA Micro Kit or from PBMCs or T cells positively selected from PBMCs using the QIAamp DNA Mini Kit, both according to the manufacturer's protocol (QIAGEN). ImmunoSEQ high-throughput *TCRB* sequencing was performed (Adaptive Biotechnologies).

Immunohistochemistry. FFPE skin sections (5–6 μm) from 5 retrospective skin-cohort patients were stained via immunohistochemistry for TCR δ clone H-41 (Santa Cruz Biotechnologies) following EDTA antigen retrieval or beta F1 clone 8A3 (Thermo Fisher Scientific) following enzyme antigen retrieval with Carezyme III: Pronase Kit (Biocare Medical). Slides were developed with 3,3′-DAB.

Laser-capture microscopy for $CD3^+$ T cells. FFPE skin sections (10 μm) from a retrospective skin-cohort patient were stained via immunohistochemistry for CD3 (LN10, NCL-L-CD3-565, Leica Biosystems) with DAB following acidic antigen retrieval. $CD3^+$ cells were isolated using a PALM MicroBeam Laser Capture Microscope with PALM RoboSoftware (ZEISS). DNA was extracted from the collected material using the QIAamp DNA FFPE Tissue Kit according to the manufacturer's instructions (QIAGEN).

STR analysis. For the skin cohort, DNA from T cells isolated from skin and peripheral blood were analyzed via STR analysis using Promega's Powerplex 21 System (Promega Corporation) with subsequent run on an ABI 3130 Genetic Analyzer (Thermo Fisher Scientific).

For the colon cohort, chimerism was performed by the Department of Forensic Medicine, Oslo University Hospital, as part of routine analysis following HSCT. PCR amplification and STR analysis were performed using the Promega PowerPlex Fusion 6C System (Promega Corp.).

IF. FFPE skin sections 5 to 6 μm thick were baked, deparaffinized, and rehydrated. Skin sections underwent acidic antigen retrieval at 96°C and were blocked for nonspecific protein binding, then stained for mouse anti-human CD3 with either anti-human Ki67 (SP6, catalog ab16667, Abcam), IL-17 (polyclonal, catalog LS-C104427, LifeSpan Biosciences), or IFN-γ (polyclonal, catalog ab25101, Abcam),

followed by secondary staining with different combinations of anti-rabbit (Poly4064, catalog 406412, BioLegend), mouse (Poly4053, catalog 405324, BioLegend), or goat (catalog A21432, Invitrogen/Thermo Fisher) IgG AF555 and/or with anti-mouse IgG AF647 (catalog A31571, Invitrogen/Thermo Fisher) or Cy2 (catalog 715-225-150, Jackson ImmunoResearch) and counterstained with DAPI. Tissue was imaged using a Mantra Quantitative Pathology Workstation and analyzed using InFORM software (PerkinElmer).

FISH-IF on FFPE tissue. FFPE skin and colon sections 5 to 6 μm thick were baked, deparaffinized, and rehydrated. Skin sections underwent acidic antigen retrieval at 96°C and pepsin treatment; colon sections underwent basic antigen retrieval at 100°C. FISH probes for X and Y chromosomes (Abbott Molecular) were hybridized overnight at 37°C. Skin sections required denaturation at 94°C before hybridization. After posthybridization washing, skin sections were blocked for nonspecific protein binding, then stained for mouse anti-human CD3 with or without rabbit anti-human CD4 (EP204, catalog AC-0173A, Epitomics), then with anti-mouse IgG AF647 (catalog A31571) with or without anti-rabbit IgG AF594 (catalog A11012, Invitrogen/Thermo Fisher) and counterstained with DAPI. Tissue was imaged using a Mantra Quantitative Pathology Workstation and analyzed using InFORM software (PerkinElmer). Colon sections were stained with rabbit anti-human CD3 (polyclonal, catalog A045201, DAKO/Agilent), mouse anti-human CD8 (4B11, catalog NCL-L-CD8-4B11, Novocastra), mouse anti-human HLA-DR (TAL.1B5, catalog M074601, DAKO), and/or mouse anti-human Ki67 (MIB-1, catalog sc-101861, Santa Cruz Biotechnology) and secondary antibodies for anti-rabbit IgG AF647 (catalog A31573) and AF555 (catalog A31572), anti-mouse IgG2b AF555 (catalog A21147), anti-mouse IgG1 AF647 (catalog A21240), and/or anti-mouse IgG1 AF555 (catalog A21127) (all Invitrogen/Thermo Fisher). After counterstaining with Hoechst, sections were mounted with ProLong Diamond. Slides were inspected by confocal microscopy, Olympus FV1000 (Olympus), and analyzed digitally using ImageJ (NIH).

FISH-IF on cytospins of dermal T cells. Dermal T cells were isolated from shave skin biopsies by migration as previously described (21). Briefly, epidermal and dermal sheets were separated by digestion in 1 mg/mL dispase (Invitrogen) in RPMI (Invitrogen) for 60 minutes at 37°C. Dermal sheets were cultured in X-Vivo 10 (Cambrex) with 500 U/mL GM-CSF (Sargramostim; Durbin PLC) and migrating cells harvested onto cytospin slides after 60 to 82 hours. Cytospin slides were air dried and stored at –20°C before sequential IF and FISH. Slides were thawed and fixed in methanol, then stained with antibodies to CD3 (SK7, catalog 347340, BD) and Alexa Fluor 633–conjugated goat anti–mouse IgG1 (catalog A-21126, Thermo Fisher). Myeloid cells were identified with antibodies to HLA-DR-FITC (L243, catalog 347363, BD), CD14 (rabbit polyclonal, catalog ab106285, Abcam), and FXIIIA (sheep polyclonal, catalog SAF13A-AP, Enzyme Research Laboratories), as previously described (21). From 10 to 12 four-color images were acquired by confocal microscopy and assembled into montages using Photoshop CS2 (Adobe). Cytospin slides were then fixed with methanol/acetic acid (3:1) for 5 minutes, probed with CEP X/Y DNA probes (Vysis, Abbott Molecular), mounted with Vectastain containing DAPI (Vector Laboratories), and scored for X/Y hybridization.

Histologic grading of human skin and colon. For skin, a modified Lerner system (53) was used based on findings by Darmstadt et al. (54) whereby grade 2 was subdivided into 2a and 2b based on 4 or fewer dyskeratotic epidermal cells per linear mm epidermis or more than 5 dyskeratotic epidermal cells per linear mm epidermis, respectively. For gut, a modified Lerner system (53) was used based on findings by Lin et al., in which patients with 2–5 crypt apoptotic bodies per 10 contiguous crypts that had typical clinical signs of GVHD were defined as histologic grade 1 (55).

Human engrafted mouse studies: human skin and blood samples. Blood from healthy individuals was obtained after leukapheresis. Skin from healthy adult patients was obtained from patients undergoing cosmetic surgery procedures, and neonatal foreskin was obtained from infants circumcised at Brigham and Women's Hospital.

Isolation of CD25-depleted PBMCs and monocytes from human peripheral blood. Magnetic-activated cell sorting (MACS) was used to prepare CD25-depleted PBMCs and purified monocytes for injection. CD25-depleted PBMCs were prepared by negative selection, and $CD14^+$ monocytes were prepared by positive selection. Briefly, cells were resuspended in cold separation buffer (PBS; Corning, containing 0.5% BSA and 2 mM EDTA; both from MilliporeSigma), incubated for 15 minutes at 4°C with anti-CD25 or anti-CD14 microbeads (Miltenyi Biotec), washed by adding 5 mL of separation buffer, and centrifuged at 300 *g* for 10 minutes. Cells were resuspended in 500 μL of separation buffer and applied onto an autoMACS Pro (Miltenyi Biotec) instrument for magnetic separation. The negative eluted fraction was used for CD25-depleted PBMCs, and the positive eluted fraction was used for monocyte separations.

Human engrafted mouse model. Adult human skin thinned with an electric dermatome or full-thickness neonatal foreskin was grafted onto the backs of 6- to 8-week-old female and male nonobese diabetic/severe combined immunodeficient/IL-2 receptor γ $chain^{null}$ mice (NSG, Jackson Laboratory). Three weeks later, (a) saline solution, (b) 5×10^6 allogeneic CD25-depleted PBMCs, or (c) 5×10^6 allogeneic monocytes were injected into mice via retroorbital injection. Skin grafts were harvested for analysis 3 weeks after injection of cells.

Immunohistochemical studies. H&E stains were carried out on FFPE tissue sections (4 μm) by standard immunohistochemical techniques.

RNA isolation and quantitative real-time PCR. Total RNA was extracted from skin grafts using the RNeasy Lipid Tissue Kit (QIAGEN). The concentration and purity of the isolated RNA was determined using a NanoDrop instrument (Thermo Scientific). Total RNA was reverse transcribed to cDNA using the SuperScript VILO cDNA Synthesis Kit (Life Technologies). Quantitative real-time PCR was performed using the ABI StepOnePlus instrument and Fast SYBR Green Master Mix (Applied Biosystems). Expression of each gene transcript was determined relative to the housekeeping gene transcript b-actin and calculated as $2^{-(Ct\ transcript\ -\ Ct\ B\text{-}actin)}$. Primer pairs were purchased from Integrated DNA Technologies. The primer sequences were as follows: *CD3E*: forward, GGGGCAAGAT-GGTAATGAAG; reverse, CCAGGATACTGAGGGCATGT; *IL-9*: forward, TCTGGTGCAGTT-GTCAGAGGGAAT; reverse, TGCAGGAAGATCCAGCTTCCAAGT; *IL-17A*: forward, CCACGAAATCCAGGATGCCCAAAT; reverse, ATT-CCAAGGTGAGGTGGATCGGTT; *IL-22*: forward, AAGGTGCGGTTG-GTGATATAG; reverse, CACCAGTTGCTCGAGTTAGAA; *IFNG*: forward, CTCTTCGACCTCGAAACAGC; reverse, TGACCAGAGCATC-CAAAAGA; *TNFA*: forward, GCCAGAGGGCTGATTAGAGA; reverse, TCAGCCTCTTCTCCTTCCTG; B-actin: forward, TCACCCACACTGT-GCCCATCTACGA, reverse, CAGCGGAACCGCTCATTGCCAATGG.

Statistics. Clonality studies were analyzed using immunoSEQ Analyzer. The remaining studies were analyzed using GraphPad Prism. Comparison of 2 independent groups was performed using Mann-Whitney *U* test, either 1-tailed or 2-tailed (specified for each analysis in the Results section and figure legends). Paired specimens were analyzed using 2-tailed Wilcoxon's signed rank test. One-way Kruskal-Wallis test was used with Dunn's post test for comparing more than 2 independent groups. Simple linear regression was used when both independent and dependent variables were continuous. A *P* value of less than 0.05 was considered significant for all statistical tests used.

Study approval. All patient studies were approved by each participating institution's ethics committee and in accordance with the Declaration of Helsinki. All tissues were collected and used with prior approval from the Institutional Review Boards of the Partners Human Research Committee (Partners Research Management), Newcastle and North Tyneside Local Research Ethics Committee 1, and the Norwegian Regional Committee for Medical Research Ethics. Written, informed consent was obtained from each patient. Animal experiments were performed in accordance with the guidelines put forth by the Center for Animal Resources and Comparative Medicine at Harvard Medical School, and all protocols and experimental plans were approved by the Harvard Medical School IACUC beforehand.

Author contributions

SJD, ATA, TRM, CPE, PCH, MH, JH, GSP, MC, and ESB performed experiments. SJD, ATA, CPE, JTO, ELM, GSP, VTH, RJS, ESB, TGD, HR, JWL, HTK, MCM, MC, JR, IG, CSC, RAC, FLJ, and TSK contributed to study design and/or analysis and interpretation of data. SJD, ATA, MC, RAC, FLJ, and TSK drafted the manuscript. Each of the 3 first authors, SJD, ATA, and TRM, contributed key data to the overall manuscript. The order of first authorship was determined based on degree of work contributed both in the laboratory and in preparation of the manuscript, with SJD contributing the most, then ATA, then TRM.

Acknowledgments

The authors would like to thank the Brigham and Women's Hospital Cytogenetics core facility, the Harvard Medical School Neurobiology imaging unit, Zihou Yan for his assistance acquiring medical record data, and David Chiluiza for his assistance in reviewing the manuscript. The authors would also like to thank Kjersti Thorvaldsen Hagen for her assistance in preparing slides for immunohistochemistry and Margurethe Rødhammer Stenersen, Norwegian Institute of Public Health, who analyzed STR analysis from the retrospective gut cohort data. This work was supported by the NIH (DP5OD023091 and T32AR007098 to SJD; R01AR065807 and R01AI127654 to TSK; R01CA203721 and P30AR069625 to RAC), the Dermatology Foundation Physician-Scientist Career Development Award (to SJD), a PhD grant from the South Eastern Norway Regional Health Authority (to FLJ), and by the Research Council of Norway through its Centres of Excellence funding scheme (project number 179573/V40 to FLJ).

Address correspondence to: Thomas S. Kupper, Harvard Institutes of Medicine, Room 673, 77 Avenue Louis Pasteur, Boston, Massachusetts 02115, USA. Phone: 617.525.5550; Email: tkupper@bwh.harvard.edu. Or to: Frode L. Jahnsen, A3.M023, Department of Pathology, Sognvannsveien 20, Rikshospitalet, 0372 Oslo, Norway. Phone: 47.23071444; Email: f.l.jahnsen@medisin.uio.no. Or to: Rachael A. Clark, EBRC Room 505A, 221 Longwood Avenue, Boston, Massachusetts 02115, USA. Phone: 617.962.3386; rclark@bwh.harvard.edu.

1. Tanaka Y, et al. Analysis of non-relapse mortality and causes of death over 15 years following allogeneic hematopoietic stem cell transplantation. *Bone Marrow Transplant*. 2016;51(4):553–559.
2. Anasetti C, et al. Peripheral-blood stem cells versus bone marrow from unrelated donors. *N Engl J Med*. 2012;367(16):1487–1496.
3. Flowers ME, et al. Comparative analysis of risk factors for acute graft-versus-host disease and for chronic graft-versus-host disease according to National Institutes of Health consensus criteria. *Blood*. 2011;117(11):3214–3219.
4. Inamoto Y, et al. Association of severity of organ involvement with mortality and recurrent malignancy in patients with chronic graft-versus-host disease. *Haematologica*. 2014;99(10):1618–1623.
5. Pasquini MC. Impact of graft-versus-host disease on survival. *Best Pract Res Clin Haematol*. 2008;21(2):193–204.
6. Jagasia M, et al. Risk factors for acute GVHD and survival after hematopoietic cell transplantation. *Blood*. 2012;119(1):296–307.
7. Magenau J, Runaas L, Reddy P. Advances in understanding the pathogenesis of graft-versus-host disease. *Br J Haematol*. 2016;173(2):190–205.
8. Zeiser R, Blazar BR. Acute graft-versus-host disease - biologic process, prevention, and therapy. *N Engl J Med*. 2017;377(22):2167–2179.
9. Pallett LJ, et al. IL-2^{high} tissue-resident T cells in the human liver: Sentinels for hepatotropic infection. *J Exp Med*. 2017;214(6):1567–1580.
10. Stelma F, et al. Human intrahepatic CD69+CD8+ T cells have a tissue resident memory T cell phenotype with reduced cytolytic capacity. *Sci Rep*. 2017;7(1):6172.
11. Sathaliyawala T, et al. Distribution and compartmentalization of human circulating and tissue-resident memory T cell subsets. *Immunity*. 2013;38(1):187–197.
12. Clark RA, et al. The vast majority of CLA+ T cells are resident in normal skin. *J Immunol*. 2006;176(7):4431–4439.
13. Purwar R, Campbell J, Murphy G, Richards WG, Clark RA, Kupper TS. Resident memory T cells (T(RM)) are abundant in human lung: diversity, function, and antigen specificity. *PLoS ONE*. 2011;6(1):e16245.
14. Park CO, Kupper TS. The emerging role of resident memory T cells in protective immunity and inflammatory disease. *Nat Med*. 2015;21(7):688–697.
15. Schenkel JM, Masopust D. Tissue-resident memory T cells. *Immunity*. 2014;41(6):886–897.
16. Clark RA. Resident memory T cells in human health and disease. *Sci Transl Med*. 2015;7(269):269rv1.
17. Iriki H, et al. Toxic epidermal necrolysis in the absence of circulating T cells: a possible role for resident memory T cells. *J Am Acad Dermatol*. 2014;71(5):e214–e216.
18. Robins HS, et al. Comprehensive assessment of T-cell receptor beta-chain diversity in alphabeta T cells. *Blood*. 2009;114(19):4099–4107.
19. Carnevale-Schianca F, et al. Longitudinal assessment of morbidity and acute graft-versus-host disease after allogeneic hematopoietic cell transplantation: retrospective analysis of a multicenter phase III study. *Biol Blood Marrow Transplant*. 2009;15(6):749–756.
20. Norton J, al-Saffar N, Sloane JP. An immunohistological study of gamma/delta lymphocytes in human cutaneous graft-versus-host disease. *Bone Marrow Transplant*. 1991;7(3):205–208.
21. Haniffa M, et al. Differential rates of replacement of human dermal dendritic cells and macrophages during hematopoietic stem cell transplantation. *J Exp Med*. 2009;206(2):371–385.
22. Busca A, Aversa F. In-vivo or ex-vivo T cell depletion or both to prevent graft-versus-host disease after hematopoietic stem cell transplantation. *Expert Opin Biol Ther*. 2017;17(11):1401–1415.
23. Clark RA, et al. Skin effector memory T cells do not recirculate and provide immune protection in alemtuzumab-treated CTCL patients. *Sci Transl Med*. 2012;4(117):117ra7.
24. Watanabe R, et al. Human skin is protected by four functionally and phenotypically discrete populations of resident and recirculating memory

T cells. *Sci Transl Med*. 2015;7(279):279ra39.
25. Jardine L, et al. Donor monocyte–derived macrophages promote human acute graft-versus-host disease. *J Clin Invest*. 2020;130(9):4574–4586.
26. Clark RA, et al. A novel method for the isolation of skin resident T cells from normal and diseased human skin. *J Invest Dermatol*. 2006;126(5):1059–1070.
27. Norton J, al-Saffar N, Sloane JP. Immunohistological study of distribution of gamma/delta lymphocytes after allogeneic bone marrow transplantation. *J Clin Pathol*. 1992;45(11):1027–1028.
28. Mavers M, Maas-Bauer K, Negrin RS. Invariant natural killer T cells as suppressors of graft-versus-host disease in allogeneic hematopoietic stem cell transplantation. *Front Immunol*. 2017;8:900.
29. Korngold R, Sprent J. Lethal graft-versus-host disease after bone marrow transplantation across minor histocompatibility barriers in mice. Prevention by removing mature T cells from marrow. *J Exp Med*. 1978;148(6):1687–1698.
30. Anderson BE, McNiff JM, Matte C, Athanasiadis I, Shlomchik WD, Shlomchik MJ. Recipient CD4+ T cells that survive irradiation regulate chronic graft-versus-host disease. *Blood*. 2004;104(5):1565–1573.
31. Blazar BR, et al. Host T cells resist graft-versus-host disease mediated by donor leukocyte infusions. *J Immunol*. 2000;165(9):4901–4909.
32. Beura LK, et al. Normalizing the environment recapitulates adult human immune traits in laboratory mice. *Nature*. 2016;532(7600):512–516.
33. Bleakley M, et al. Outcomes of acute leukemia patients transplanted with naive T cell-depleted stem cell grafts. *J Clin Invest*. 2015;125(7):2677–2689.
34. Andreani M, et al. Persistence of mixed chimerism in patients transplanted for the treatment of thalassemia. *Blood*. 1996;87(8):3494–3499.
35. Andreani M, et al. Long-term survival of exthalassemic patients with persistent mixed chimerism after bone marrow transplantation. *Bone Marrow Transplant*. 2000;25(4):401–404.
36. Sachs DH, Kawai T, Sykes M. Induction of tolerance through mixed chimerism. *Cold Spring Harb Perspect Med*. 2014;4(1):a015529.
37. Walters MC, et al. Stable mixed hematopoietic chimerism after bone marrow transplantation for sickle cell anemia. *Biol Blood Marrow Transplant*. 2001;7(12):665–673.
38. Bartolomé-Casado R, et al. Resident memory CD8 T cells persist for years in human small intestine. *J Exp Med*. 2019;216(10):2412–2426.
39. Snyder ME, et al. Generation and persistence of human tissue-resident memory T cells in lung transplantation. *Sci Immunol*. 2019;4(33):eaav5581.
40. Nakamura H, Gress RE. Graft rejection by cytolytic T cells. Specificity of the effector mechanism in the rejection of allogeneic marrow. *Transplantation*. 1990;49(2):453–458.
41. Kernan NA, Flomenberg N, Dupont B, O'Reilly RJ. Graft rejection in recipients of T-cell-depleted HLA-nonidentical marrow transplants for leukemia. Identification of host-derived antidonor allocytotoxic T lymphocytes. *Transplantation*. 1987;43(6):842–847.
42. Voogt PJ, et al. Rejection of bone-marrow graft by recipient-derived cytotoxic T lymphocytes against minor histocompatibility antigens. *Lancet*. 1990;335(8682):131–134.
43. Ho VT, Soiffer RJ. The history and future of T-cell depletion as graft-versus-host disease prophylaxis for allogeneic hematopoietic stem cell transplantation. *Blood*. 2001;98(12):3192–3204.
44. Buggins AG, et al. Peripheral blood but not tissue dendritic cells express CD52 and are depleted by treatment with alemtuzumab. *Blood*. 2002;100(5):1715–1720.
45. Fabian I, Flidel O, Gadish M, Kletter Y, Slavin S, Nagler A. Effects of CAMPATH-1 antibodies on the functional activity of monocytes and polymorphonuclear neutrophils. *Exp Hematol*. 1993;21(12):1522–1527.
46. Jin F, et al. Antithymocyte globulin treatment at the time of transplantation impairs donor hematopoietic stem cell engraftment. *Cell Mol Immunol*. 2017;14(5):443–450.
47. Herve P, et al. Removal of marrow T cells with OKT3-OKT11 monoclonal antibodies and complement to prevent acute graft-versus-host disease. A pilot study in ten patients. *Transplantation*. 1985;39(2):138–143.
48. Chinn IK, Shearer WT. Severe combined immunodeficiency disorders. *Immunol Allergy Clin North Am*. 2015;35(4):671–694.
49. Díaz de Heredia C, et al. Unrelated cord blood transplantation for severe combined immunodeficiency and other primary immunodeficiencies. *Bone Marrow Transplant*. 2008;41(7):627–633.
50. Dinardo L, Brown V, Perez E, Bunin N, Sullivan KE. A single-center study of hematopoietic stem cell transplantation for primary immune deficiencies (PIDD). *Pediatr Transplant*. 2012;16(1):63–72.
51. Sato T, et al. Stem cell transplantation in primary immunodeficiency disease patients. *Pediatr Int*. 2007;49(6):795–800.
52. Tsuji Y, et al. Hematopoietic stem cell transplantation for 30 patients with primary immunodeficiency diseases: 20 years experience of a single team. *Bone Marrow Transplant*. 2006;37(5):469–477.
53. Lerner KG, Kao GF, Storb R, Buckner CD, Clift RA, Thomas ED. Histopathology of graft-vs.-host reaction (GvHR) in human recipients of marrow from HL-A-matched sibling donors. *Transplant Proc*. 1974;6(4):367–371.
54. Darmstadt GL, Donnenberg AD, Vogelsang GB, Farmer ER, Horn TD. Clinical, laboratory, and histopathologic indicators of the development of progressive acute graft-versus-host disease. *J Invest Dermatol*. 1992;99(4):397–402.
55. Lin J, Fan R, Zhao Z, Cummings OW, Chen S. Is the presence of 6 or fewer crypt apoptotic bodies sufficient for diagnosis of graft versus host disease? A decade of experience at a single institution. *Am J Surg Pathol*. 2013;37(4):539–547.